REGISTRATION OF RENAL SPECT AND 2.5D US IMAGES

Francisco J. GALDAMES[1,2], Claudio A. PÉREZ[1], Pablo A. ESTÉVEZ[1], Claudio M. HELD[1], Fabrice JAILLET[2], Gabriel LOBO[3], Gilda DONOSO[3], Claudia COLL[3]

(1) Department of Electrical Engineering – Universidad de Chile – Av. Tupper, 2007 – Santiago – Chile
(2) LIRIS-SAARA – UMR CNRS 5205 – Université Lyon 1 – Villeurbanne – F-69622 – France
(3) Medicina Nuclear – Hospital San Juan de Dios – Santiago – Chile
Correspondent author: fgaldame@ing.uchile.cl

The main goal of this study is the registration of renal SPECT (Single Photon Emission Computerized Tomography) and 2.5D US (Ultrasound) images. In the proposed approach, the matching is performed after kidney segmentation in both images. The SPECT segmentation is achieved using a deformable model based on a simplex mesh. And the 2.5D US image segmentation is carried out in every 2D slice by mean of a deformable contour. Next, the registration is carried out using a nonlinear optimization algorithm, and this registration was also used to correct the movements in the US image caused by the patient respiration during acquisition. The registration was evaluated quantitatively comparing the distance between a manual segmentation in the US image and the model extracted from de SPECT image. Qualitative expertise is currently been realized.

INTRODUCTION

In the current clinical procedure, the use of medical images for diagnosis, planning, evaluation, and treatment settings is of essential importance. Within this study, the main goal is the registration of renal SPECT and 2.5D US images. SPECT images are extremely valuable in the diagnosis of various renal disorders. However, uncertainty in the anatomic definition on SPECT may limit their usefulness: often, there isn't enough anatomical detail to determine the position of a lesion. To overcome this problem, integration with structural images of the kidneys is used to impose anatomical information on the functional one.

Image registration is the process of transforming different sets of data into the same coordinate system [9]. The first approach is to use fiducial marks visible in both images. This is efficient, but very invasive. Some devices permit to

acquire two image modalities at the same time, leading to an obvious registration stage, but unfortunately at excessive cost. Finally, an alternative approach is to achieve a registration only based on image contents.

In the literature, few works deal with registration between SPECT and 2.5D US images. Examples are described in [2,10], nevertheless it was carried out with help of an optical position sensor. Other example of similar kind of registration between MR and a sparse set of US slices has been achieved using the probability of existence of vessels [14]. There are also works on registration of US and MR using intensity and gradient information [15] or between US images [16] using a correlation measurement like mutual information. In our approach, the registration is carried out by performing a matching of previous segmentations of the kidneys in both images.

This paper is organized as follows: Section 1 and 2 present the acquisition and segmentation steps respectively for SPECT and 2.5D US images, including an evaluation of the segmentation. In Section 3, the registration algorithm is explained, and some quality evaluations are presented. Finally, a discussion and some perspectives of the work are exposed.

1. THE SPECT MODALITY

The first step of our SPECT/US registration task is to perform a segmentation of the kidneys in the functional image. The SPECT images were obtained injecting Tc-99m DMSA. This radioactive isotope is transported by blood and will be fixed by the renal cortex, thus exhibiting kidneys perfusion and function. A set of images are taken at different projection angles through a dual-head (SMV DST-Xli) gamma camera acquisition. 3D images were reconstructed by the OSEM (Ordered Subsets Expectation Maximization) iterative method, using 64 projections at 180º. The images size was 128x128x128 with 4x4x4mm voxels.

1.1. SPECT Segmentation

The SPECT segmentation of the kidneys is achieved using a deformable model method because of its robustness and high noise immunity [12]. A simplex mesh [4] that is iteratively adjusted to the shape of the kidney has been chosen for the model implementation. This mesh has been successfully applied to the segmentation of cardiac SPECT images [13], and in a previous work on renal segmentation [6].

In a simplex mesh, the position of each vertex is expressed according to the position of its 3 neighbors and some shape parameters. Deformation is thus very easily handled by discrete geometric entities. Dynamics of the model is controlled by means of a Newtonian law of motion:

$$m\frac{\partial^2 P_i}{\partial t^2} = -\gamma\frac{\partial P_i}{\partial t} + \lambda\overrightarrow{F_{\text{int}}} + \kappa\overrightarrow{F_{ext}}, \quad (1)$$

where m the vertex mass unit (usually 1), P_i the vertex position, γ the damping factor, F_{int} internal forces extracted from the mesh (to obtain a smooth deformation), F_{ext} external forces

extracted from the image (to push the mesh towards the borders), κ and λ weighting associated to the forces.

The first step is to define a mesh around each kidney. The initial isosurface is determined by the "marching tetrahedra" algorithm [18]. Then, the simplex mesh is obtained directly from the topological dual of this triangulation.

Two types of mesh deformations were tested, that can be differentiated by the external forces field they use. The first one was based on image gradient using the GVF (Gradient Vector Flow) algorithm [21]. Thus, borders are located in areas of high gradient characteristics. The other type of mesh deformation was based on voxels intensity to obtain a result similar to an isosurface but smoothed because of the mesh rigidity. For this, the external forces field was obtained using central differences in a smoothed binary image of the kidneys.

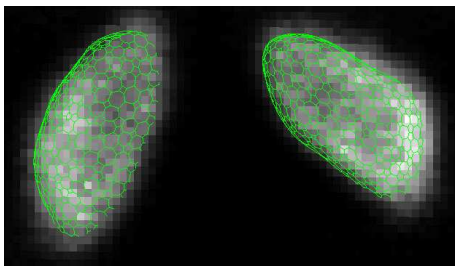

Fig. 1: SPECT image segmented by a simplex mesh

1.2. Evaluation of SPECT Segmentation

Evaluations for both gradient and intensity SPECT segmentation were carried out on 27 exams, which were part of routine examinations ordered by physicians. Parameters used for the model dynamics were empirically set as: κ=0.8, λ=0.2, γ=0.65.

Using a graphic interface the segmentations were evaluated qualitatively by a medical experts commission. The evaluation range was from 1 to 5 (1: very bad, 2: bad, 3: good, 4: very good, 5: excellent [19]). For all images, the gained score was 5.

Thus, according to experts, both methods exhibit equivalent results and are acceptable. At this step, none method can be qualitatively differentiated. However, registration results, in Section 3, will permit to discriminate which edge definition is the more appropriate in the experts' opinion.

Finally, it might be interesting to evaluate quantitatively these segmentations, for example, by comparing with phantoms or with a localized registration [10].

2. THE 2.5D US MODALITY

The second step in the whole registration process is to segment the kidneys in the anatomical data. Thanks to an optical localizer (Praxim Surgetics® station) permitting to track the position of a rigid body fixed to the US probe [7], the considered 2.5D US images are composed of a set of freehand 2D US images with associated spatial coordinates. Each US image was obtained using an echo camera Aloka 55D-630 at resolution 480x640 with a 0.25x0.19mm pixel size.

2.1. Segmentation of 2.5D US

The 2.5D US image segmentation process is conducted separately in each slice of the 2D images set. This 2D segmentation is performed by mean of a deformable contour method, using a set of Gabor filters to capture image features in multiscale.

Although deformable contours have high noise immunity, they are very sensitive to the initialization. Furthermore, compared with other medical imaging modalities, US images are particularly difficult to segment [11, 20] since their quality is relatively low, with significant noise even in very bright regions. Moreover, the tissue-tissue boundaries of kidney are relatively more difficult to localize in US image than for other organs, and previous studies have shown that even a manual segmentation is not straightforward. Thus, to achieve an automatic segmentation is not an easy task, leading to the necessity of a manual initialization.

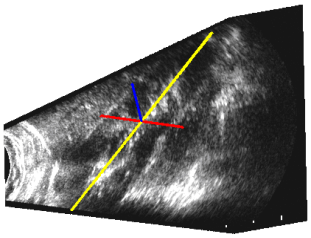

Fig. 2 : Manual localization of the ellipsoid axes coincident to the kidney ones in 3D

The initialization consists in positioning an ellipsoid in the kidney location. Thus, the user intervention simply results in identifying the principal axes of the kidney (axial, and sagittal or coronal) in a US image. This initialization is realized by choosing a central slice of the kidney, and next rotating, scaling and moving 2 axes in the image, the third one being automatically deduced thanks to symmetry. If both kidneys appear in the 2.5D US image then one ellipsoid is positioned for each kidney. Fig. 2 shows an US slice and the 3D position of the ellipsoid axes.

In the literature, Gabor functions have often been used for the segmentation of US images [17, 20] due to their appropriate texture characterization. Here, we used circular functions to capture image features in multiscale. After experimenting various frequencies, the set of central frequencies of the Gabor functions have been selected empirically to $F=\{0.08, 0.2, 0.35\}$; and the usual $\theta=\{0, \pi/6, \pi/3, \pi/2, 2\pi/3, 5\pi/6\}$ set of angles has been used (covering 180° degrees) as in [20].

Next, the filtering step is performed to obtain a set of images $E_{F,\theta}$ for every 2D US image, where F is the radial center frequency and θ the Gabor filter angle. Using this image set, borders of the kidney are searched with help of active contours [3, 8, 12]. For this, the contour is defined by a set of points $\{P_i\}_{i=1}^{N_P}$. The dynamics of each vertex is given by a Newtonian law of motion, like in eq. (1), and the internal force is defined as:

$$F_{\text{int}}(i) = \alpha \frac{\partial^2 U(i)}{\partial i^2} - \beta \frac{\partial^4 U(i)}{\partial i^4}, \quad (2)$$

where α and β are weights that control tension and rigidity of the curve, respectively.

In order to obtain a more appropriate field of external forces (smooth and without undesired locals minima), the GVF algorithm [21] is used. Moreover, we need to eliminate forces corresponding to the renal medulla, because otherwise they may attract the contour that falls in a local minimum, leading to incorrect border determination. Three edge maps, obtained from the $E_{F,\theta}$ images calculated with the three central frequencies, are introduced to the GVF algorithm. Thus, three force fields are obtained, that permit to carry out a coarse-to-fine deformation (from the lowest to the highest frequency).

As initial contour for each 2D US image, we use the resultant ellipse of the intersection between this image and the previously defined initial ellipsoid. We apply affine transformations to this ellipse to better match the kidney borders. This adjustment was carried out maximizing the integration, along the ellipse, of the filtered image gradient in the direction normal to the ellipse. This way, the vector $\hat{p} = [\hat{\alpha}, \hat{s}, \hat{t}]$ of the optimal rotation $\hat{\alpha}$, scaling $\hat{s}$, and translation $\hat{t}$, is obtained for each ellipse, with:

$$\hat{p} = \underset{\alpha,s,t}{\operatorname{argmax}} \sum_{i}^{N_P} \nabla E_{F\theta}(T(P_i;p)) \cdot N(T(P_i;p)) \quad (3)$$

where $\nabla E_{F\theta}$ is the gradient of the filtered image, $N(P_i)$ is the normal to the ellipse at point P_i, and $T(\cdot;p)$ is the transformation with vector of parameters p. Thus, the resultant ellipse is deformed using the forces field obtained with the minimum frequency Gabor filter. Then, the resultant contour is deformed sequentially with the other force fields, carrying out a coarse-to-fine approximation. The dynamics of the contour were controlled by means of eq. (1).

After the deformation step, only some of the points P_i are kept, ie. the ones with a value m_i in the edge map f_F with maximal frequency greater than 20% of the maximal value. These curve segments are united if they have a separation smaller than a threshold (30 pixels approx.). Finally, all the small curve segments are eliminated, providing with highly confident border segments. Fig. 3 illustrates the final result of the whole US segmentation process.

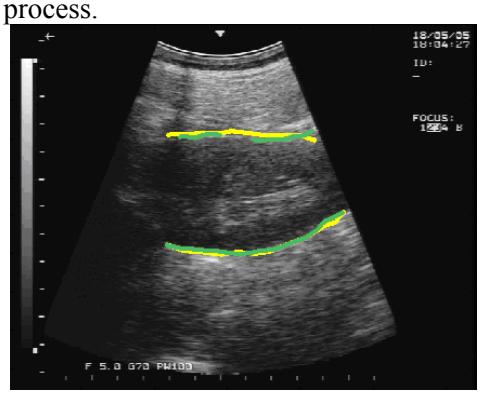

Fig. 3 : Superposition of automatic (green) and manual (yellow) US segmentation.

2.2. Evaluation of US Segmentation

For the evaluation of the segmentation, it was taken a 2.5D US to one patient and two volunteers. The used parameters were empirically selected as: κ=10, α=0.6, β=0, γ=0.65, λ=1.

It was requested to medical experts to mark the kidney borders in each one of the 2D images by help of a graphic interface. They only delineated those borders they can clearly identify. The

distance between this manual segmentation and the semi-automatic one issued from our method has been measured. Table 1 shows the percentage of images in which the initial ellipse was not positioned correctly (in those images, the distance was not measured), the average distance, and the percentage of borders found in comparison to the manual segmentation. Results exhibit the good behavior of our method, leading to detecting the kidney edges with a precision of approximately 1.5 mm. For patient B, initialization failed for several images, mostly for those lying at the extremities of the kidney or because of highly noisy.

Table 1 : Results of our US segmentation according to manual contouring.

Patients	A	B	C
bad initialized images [%]	0.0	18.0	4.1
Average distance [pix]	5.09	11.06	7.18
Edges found [%]	60.86	77.10	79.46

3. REGISTRATION

For the registration of the structures found in both images, a nonlinear optimization algorithm is used [5]. Furthermore, this registration is also used to correct the movements in the 2.5D US image caused by the patient respiration during acquisition, leading to an accurate global localization of the kidney in each slice.

First, a pre-registration is made with a similarity transformation (gravity centers and main directions). It is based on the position of the kidney delivered in the initialization of the 2.5D US image segmentation, and on the segmentation of the SPECT image. Next, to achieve the registration, a minimization is carried out over the quadratic distance between the points found in the 2.5D US image and the 3D kidneys model extracted from the SPECT image. During the acquisition of the 2.5D US images, movements caused by the respiration induce that the kidney position in each 2D image is slightly different. To correct this movement, it is necessary to register each US slice separately and then to realize a global registration of the 2.5D US image. Thus, iterations are realized with registrations of two types: a rigid registration for every slice and a general registration using a similarity transformation. The parameters of the similarity transformation are three rotation angles, three translations, and one scale parameter. This process is repeated until the mean movement of the points found in the 2.5D US image is less than 0.5 pixels. Levenberg-Marquardt algorithm, optimized by the distance transform, was used for the minimization of the quadratic distance. This implementation is comparable with the popular ICP algorithm [1, 5]. Fig. 4(a) shows the 3D kidneys model and the points found in the 2.5D US image, after registration. Fig. 4(b) shows a SPECT/US registration example.

3.1. Evaluation of the Registration

Registration was achieved on the same set of patient than in section 2.2. In the quantitative evaluation, distance after registration between the 3D model extracted from the SPECT image and the manual contouring in the US image

has been measured. As the registration process tries to align the kidney borders in both images, this can be considered as a quality measure of the registration. Table 2 shows the average distances for both gradient and intensity SPECT segmentation. The results are of good quality, and show similar performance for both SPECT segmentations.

Table 2. Quantitative registration evaluation	
Type of SPECT segmentation	Average distance [mm]
gradient	3,24
intensity	3,30

In a previous study, medical experts have been evaluating the same registration method, but without the correction of the US localization, with a poor 3.13 average score over a 1 to 5 range. A new expertise is currently being realized. And as it was the case for the quantitative one, we are confident in obtaining better results.

4. CONCLUSIONS

A method was developed in order to register renal SPECT and 2.5D US images. The method is based on a previous segmentation of the images. The SPECT segmentation, 2.5D US segmentation and registration, were evaluated separately. Results show that the registration was successfully performed. However its quality could be improved. Our method take into account movements due to respiration, registering each 2D US image, but important enhancement can be achieved through better acquisition protocol to reduce movements of the kidneys during the acquisition phase. Moreover, we believe that the introduction of priors shape of the expected anatomical structure will be a significant advantage during the segmentation process, leading thus to a better registration. From the medical point of view, it may also be useful to have an objective automatic correlation between lesions seen in the SPECT with what appears in the US, for example the ratio between functional lesions and volume of the kidney.

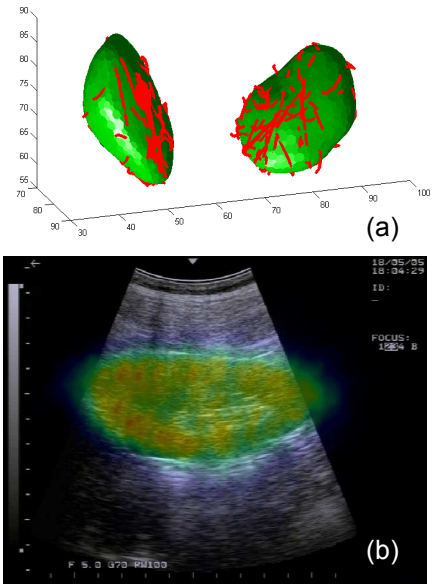

Fig. 4 : (a) 3D kidneys model and the points found in the 2.5D US image, after the registration. (b) Example of SPECT/US images registration.

Acknowledgements

This research was partially funded by CONICYT through project FONDEF 1035, DIE and CMM, Universidad de Chile; and by the European project Alfa-IPECA.
All exams were taken at the San Juan de Dios hospital in Santiago, Chile.

BIBLIOGRAPHY

[1] P. J. Besl, N. McKay
A method for registration of 3-D shapes
IEEE Trans. on PAMI, February 1992, vol. 14, no. 2, pp. 239–256.

[2] J. P. Caravel, A. Francois-Joubert, O. Peria, S. Dalsoglio, D. Cordonnier, P. Cinquin
Registration of anatomical and functional images of the kidney
Médecine Nucléaire, 1995, vol. 19, no. 5-6, pp.391-396.

[3] L. D. Cohen, I. Cohen
Finite-element methods for active contour models and balloons for 2-D and 3-D images
IEEE Trans. on PAMI, Nov. 1993, vol. 15, pp. 1131 1147.

[4] H. Delingette
General Object Reconstruction based on Simplex Meshes
I.N.R.I.A., Sophia-Antipolis, France, Tech. Rep. 3111, 1997.

[5] A. W. Fitzgibbon
Robust registration of 2D and 3D point sets
Image and Vision Computing, December 2003, vol. 21, no. 13-14, pp. 1145-1153.

[6] F. J. Galdames, C. A. Perez, P. A. Estévez, C. M. Held
Segmentation of Renal SPECT Images Based on Deformable Models
SURGETICA'2005, Computer-Aided Medical Interventions: tools and applications, 2005, pp. 89-96.

[7] A. Gee, R. Prager, G. Treece, L. Berman
Engineering a freehand 3D ultrasound system
Pattern Recognition Letters, February 2003, vol. 24, no. 4-5, pp. 757–777.

[8] M. Kass, A. Witkin, D. Terzpoulos
Snakes: Active contour models
Int. J. of Computer Vision, 1987, vol. 1, no. 4, pp. 321–331.

[9] J. B. A. Maintz, M. A. Viergever
A survey of medical image registration
MedIA, 1998, vol. 2, no. 1, pp. 1–36.

[10] M. Bucki, F. Chassat, F. Galdames, T. Asahi, D. Pizarro, G. Lobo
Real-Time SPECT and 2D Ultrasound Image Registration
MICCAI 2007, to appear.

[11] M. Martín-Fernández, C. Alberola-López
An approach for contour detection of human kidneys from ultrasound images using Markov random fields and active contours
MedIA, 2005, vol. 9, pp. 1–23.

[12] T. McInerney, D. Terzopoulos
Deformable models in medical image analysis: A survey
MedIA, 1996, vol. 1, no. 2, pp. 91–108.

[13] J. Montagnat, H. Delingette
4D deformable models with temporal constraints: application to 4D cardiac image segmentation
MedIA, 2005, vol. 2, no. 1 , pp. 87-100

[14] G. P. Penney, J. M. Blackall, M. S. Hamady, T. Sabharwal, A. Adam, D. J. Hawkes
Registration of freehand 3D ultrasound and magnetic resonance liver images
MedIA, 2004, vol. 8, no. 1, pp. 81–91

[15] A. Roche, X. Pennec, G. Malandain, N. Ayache
Rigid registration of 3-D ultrasound with MR images: a new approach combining intensity and gradient information
IEEE Trans. on Medical Imaging, October, 2001, vol. 20, no. 10, pp. 1038 -1049.

[16] R. Shekhar, V. Zagrodsky
Mutual Information-Based Rigid and Nonrigid Registration of Ultrasound Volumes
IEEE Transactions on Medical Imaging, January 2002, vol. 21, no. 1, pp. 9-22.

[17] D. Shen, Y. Zhan, C. Davatzikos
Segmentation of prostate boundaries from ultrasound images using statistical shape model
IEEE Trans. on Medical Imaging, April 2003, vol. 22, no. 4, pp. 539-51.

[18] G. M. Treece, R. W. Prager, A. H. Gee
Regularised marching tetrahedra: improved iso-surface extraction
Computer & Graphics, 1999, vol. 23, no. 4, pp. 583-598.

[19] V. Walimbe, V. Zagrodsky, S. Raja, W. A. Jaber, F. P. DiFilippo, M. J. Garcia, R. C. Brunken, J. D. Thomas, R. Shekhar
Mutual information-based multimodality registration of cardiac ultrasound and SPECT images: a preliminary investigation
Int. J. of Cardiovascular Imaging, Dec. 2003, vol. 19, no. 6, pp. 483-494.

[20] J. Xie, Y. Jiang, H. T. Tsui
Segmentation of kidney from ultrasound images based on texture and shape priors
January, 2005, IEEE Trans. on Medical Imaging, vol. 24, no.1, pp. 45-57.

[21] C. Xu, J. L. Prince
Snakes, Shapes, and Gradient Vector Flow
IEEE Trans. on Image Processing, March 1998, vol. 7, no. 3, pp. 359-369.